Study of Inner Jet of Blazars

M.Sc. Thesis

By

Anuraag Arya

msc1903121009

Discipline of Astronomy, Astrophysics and Space Engineering

INDIAN INSTITUTE OF TECHNOLOGY INDORE

June 12, 2021

Study of Inner Jet of Blazar

M.Sc. Thesis

Submitted in partial fulfillment of the requirements for the awards of the degree
of
Master of Science

by

Anuraag Arya

msc1903121009

Discipline of Astronomy, Astrophysics and Space Engineering

INDIAN INSTITUTE OF TECHNOLOGY INDORE

June 12, 2021

INDIAN INSTITUTE OF TECHNOLOGY INDORE

CANDIDATE'S DECLARATION

I hereby certify that the work which is being presented in the thesis entitled **"Study of Inner Jet of Blazars"** in the partial fulfillment of the requirements for the award of the degree of MASTER OF SCIENCE in ASTRONOMY and submitted in the DEPARTMENT OF ASTRONOMY, ASTROPHYSICS AND SPACE ENGINEERING, **Indian Institute of Technology Indore**, is an authentic record of my own work carried out during the time period from July, 2020 to May, 2021 under the supervision of Dr. Amit Shukla.

The matter presented in this thesis has not been submitted by me for the award of any other degree of this or any other institute.

Anuraag Arya.
09/06/2021
Signature with date
(Anuraag Arya)

This is to certify that the above statement made by the candidate is correct to the best of my knowledge.

09-06-2021
Signature of the Supervisor of M.Sc. thesis (with date)
(Dr. Amit Shukla)

Anuraag Arya has successfully given his M.Sc. Oral Examination held on 9th June 2021

Signature(s) of Supervisor(s) of M.Sc. thesis, Date: 09-06-2021

M.Sc. Coordinator
Date:- 09-06-2021

Head of the Department
Date:- 10/06/2021

Suman Majumdar
11/06/2021
Convener, DPGC
Date:-

Signature(s) of PSPC Member 1
Date: 11.06.2021

Signature of PSPC Member 2
Date:- 11.06.2021

Abstract

Process of extraction of jet energy Blazars(AGN) is the best experimental source of highly luminous γ-ray jets. It can be investigated through the Blandford-Znajek(BZ) process, where sources are observed on average γ-ray luminosity through Fermi-LAT over 11 months of operations. Since most Blazars belong to elliptical galaxies and numbers of stars in galaxies are roughly the same, hence the effect of gravity on central SMBH will be mass-dependent, which should be related to their spin parameter(angular momentum) and based on the rotation of accreting plasma in the accretion disk, the strength of developed magnetic fields (called force-free magnetosphere) should also be spin-dependent and hence finally mass-dependent. Through the BZ process, Blazars spin parameter and magnetic fields can be estimated as a mass-dependent function. Ultimately, a phase-space of mass and luminosity can be traced for these sources, where all the sources are constrained by minimum and maximum boundary of luminosity.

Contents

List of Symbols

Space-time parameters

- Space-time Coordinates: (t, r, θ, ϕ)

- killing vector of timelike :
  k = $\frac{\delta}{\delta t}$ = (1,0,0,0)

- Azimuthal killing vectors :
  m = $\frac{\delta}{\delta \phi}$ = (0,0,0,1)

- Inherent angular velocity:
  $\omega = -k.m/m.m = -g_{t\phi}/g_{\phi\phi}$

- Black hole parameters for characterization
  Mass: M
  Angular momentum:J^H
  Maximum angular momentum:$J^H_{max} = M^2$
  Specific angular momentum: a = J^H/M
  Angular Velocity: $\Omega^H = a/(r_+^2 + a^2)$

  Units
  solar mass: $M_\odot$
  spin parameter: a (unitless)

Chapter 1

Introduction

1.1 Unification of AGNs

The Universe contains lots of things that are still mysterious. However, continuous efforts by scientists always do constructive work to understand the vast universe. Since the galaxies, the stars, the planets, the comets, the asteroids, etc., are sets of the gigantic Universe, where the luminous objects in the sky are mostly stars and galaxies. The Discovery of Black body (by Max plank) radiation explains well the properties of thermal radiation. Still, it fails to explain those galaxies, consisting of mostly some irrelevant property at the central part. Some galaxies have been observed with higher luminosity at their center, which is typically not possible through stars. Now, it has been considered that the central part of galaxies have a supermassive black hole, and among them, some are existing with the powerful jet that possesses very high luminosity, basically defined as an active galactic nucleus (shortly termed as AGN) (Shields 1999).

Since the observation of these celestial objects is based mainly on the detection of receiving photons of the sources and basic orientation of these sources, hence AGN can be categorized into three wide sorts dependent on the attributes of their optical and bright spectra.

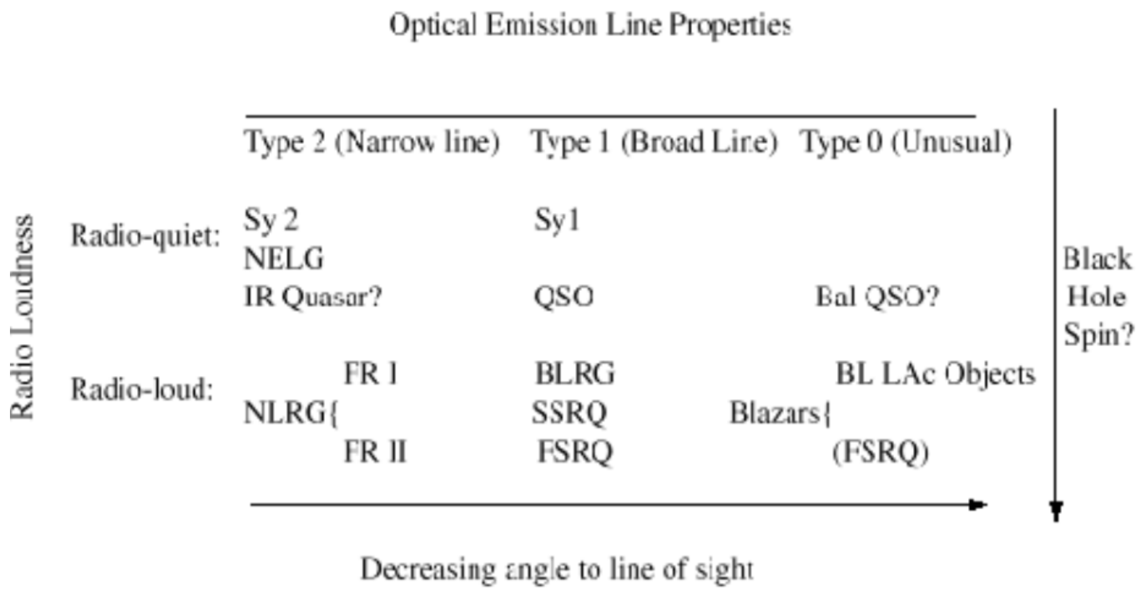

Figure 1.1: Listed table of AGNs

1. Type-1 AGN is a class of broad emission lines and the bright continua from hot high-speed gas. It is probably found somewhere down in the gravitational well of the SMBH. The radio-quiet group includes the Seyfert 1 galaxies, having relatively low-luminosities.

2. Type-2 AGN is a class of weak continua and narrow emission lines only, which implies possibly they have no high-speed gas or the view to such gas is clouded by a thick mass of retaining material. Type 2 AGN (radio-quiet) includes Seyfert 2 galaxies that belong to low luminosities. Whereas Radio-loud Type 2 AGN is called Narrow-Line Radio Galaxies (NLRG), which are additionally classified as two morphological sorts: (a) the low-glow Fanaroff-Riley type I radio cosmic systems (Fanaroff and Riley 1974)(Scaife and Porter 2021), which have often-symmetric radio jets whose intensity falls away from the nucleus. (b) the high-luminosity Fanaroff-Riley type II radio galaxies have more highly collimated jets, leading to well-defined lobes with prominent hot spots.

3. A couple of AGN have strange qualities. These are called Type 0 AGN and hypothesize that a slight angle relates with the sightline. These are the BL Lacertae (BL Lac) objects, which are radio-loud AGN with an absence of strong emission or absorption feature. All in all, generally 10% of radio-quiet AGN strangely show broad emission lines in their optical and bright spectra. These are known as BAL (Broad Absorption Line) quasars. Additionally, a subset of Type 1 quasars are known as optically violently variable (OVV) quasars, highly polarized quasars (HPQ), Center Dominated Quasar (CDQ) or FSRQ. These are found with a slight angle with the line of view. Their continuum emission strongly resembles BL Lac objects (anticipate the presence of a blue bump). Consequently, like BL Lac objects, these are additionally described by very rapid variability, unusually high and variable polarization, high brightness temperatures (often over the Compton limit T $\sim 10^{12}$ K), and superluminal velocities of compact radio cores. However, the names OVV, HPQ, CDQ, and FSRQ (flat-spectrum radio quasars) reflect their empirical definitions, FSRQ show rapid variability, high polarization, and radio structures(dominated by compact radio cores). And BL Lacs and FSRQ are collectively called blazars; see fig.(1.2) for the unified view of AGN.

1.2 Basic definitions

1.2.1 Luminosity

It is an exact physical measurement of emitted electromagnetic radiation energy per unit of time. In astronomy, the luminosity(Morison 2013) of objects is described as the electromagnetic spectrum.

1.2.2 Black Hole

According to the General theory of relativity, A black hole(Wald 2010) is a surrounded region of strong gravity(enough to trap light around horizon radius) that

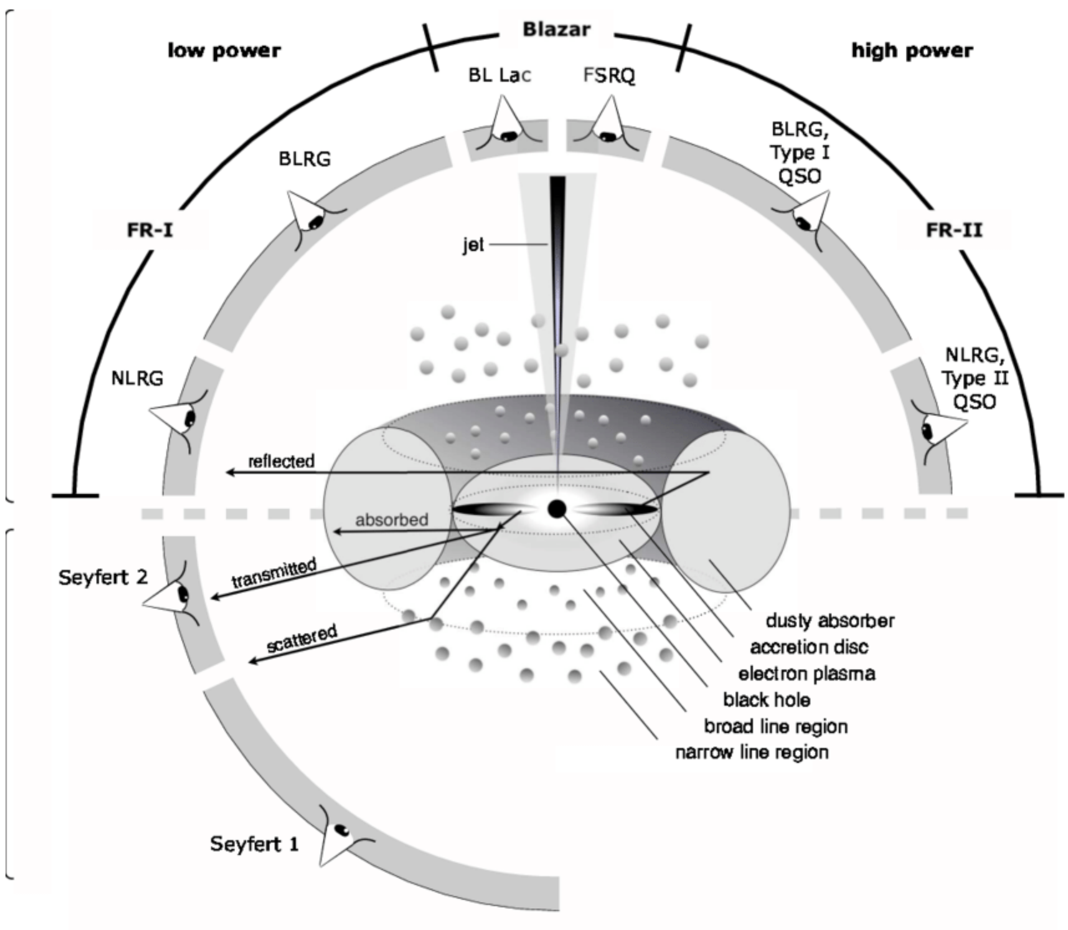

Figure 1.2: The unified view of AGN (Beckmann and SHRADER 2013)

can deform space-time around it in a complex way due to its very compact mass.

1.2.3 Schwarzschild Radius

Schwarzschild Radius is a spherical gravitational boundary around a massive object, where light photons are trapped forever beyond that region.
Mathematically,

$$\mathrm{R_{sch}} = 2\frac{GM}{c^2} \tag{1.1}$$

For a non-rotating black hole, It is called event horizon radius.

1.2.4 Eddington Luminosity

The Eddington luminosity(Marle, Owocki, and Shaviv 2008) is the maximum luminosity achieved due to the balance between the radiation pressure(outward) and gravitational pressure(inward) by a source such as stars, black holes e.t.c.

$$\mathrm{L_{Edd}} = \frac{4\pi G M_{\odot} m_p c}{\sigma_T} \tag{1.2}$$

1.2.5 Eddington Accretion Rate

The rate of accretion for which a source can radiate with Eddington luminosity.

$$\mathrm{M_{Edd}} = \frac{\mathrm{L_{Edd}}}{\epsilon_{\mathrm{rad}}\mathrm{c}^2} \tag{1.3}$$

1.2.6 Kerr Black Hole

Kerr proposed a metric of space-time(Kerr 1963) in 1963 after the development of Albert Einstein's general theory of relativity in November 1915.(Sauer 2014). Since Karl Schwarzschild solved the field equations that determine the exact space-time geometry of a non-rotating object, Where Birkhoff's uniqueness theorem (Deser and Franklin 2005) states that any spherically symmetric solution of the vacuum field equations must be static and asymptotically flat. This means that the Schwarzschild metric must give the exterior solution of the space-time outside of a spherical, non-rotating gravitating body like a black hole and the endpoint of stellar collapse

Coordinates(Oppenheimer and Snyder 1939).
The line element describes the Schwarzschild geometry.

$$ds^2 = -\left(1 - \frac{2GM}{rc^2}\right)c^2dt^2 + \frac{1}{\left(1 - \frac{2GM}{rc^2}\right)}dr^2 + r^2(d\theta^2 + \sin^2\theta d\phi^2) \tag{1.4}$$

Where M is the physical mass of the central object. But, we know that stars (also matter, planets) rotate, and hence it's a form of the weak-field approximation of the Einstein equations. Again we know the approximate condition of the metric at large distances from a stationary isolated body of mass M and angular momentum J, and it can not be approached by Schwarzschild metric in case of rotating(having angular momentum) objects (Baldwin 2021). The Kerr space-time is a more general form, whereas The Schwarzschild metric is a driven case under the zero angular momentum condition.

For the weak-field asymptotic result, it can already be seen that angular momentum destroys spherical symmetry. Which makes the calculations much more difficult algebraic complexity of the so high computations. Although it is easy to derive and check by hand the Schwarzschild solution whereas, for the Kerr space-time, the situation is somewhat different and too complex. But Chandrasekhar explains theoretical black holes(Chandrasekhar 1992) that is devoted to Kerr's algebraic complexity in his book.

1.2.7 Angular Momentum

Since the Kerr metric can describe mechanical parameters for a rotating black hole(uncharged).Where angular momentum shows a special effect called frame-dragging in space-time near the black hole. A dimensionless spin parameter has been introduced to represent the angular momentum property easily, for which their value lies between 0 (non-rotating, or Schwarzschild black hole) and 1 (maximally-rotating Kerr black hole). Mathematically,

$$\mathrm{J} = \frac{\mathrm{aGM}_\odot^2}{\mathrm{c}} \tag{1.5}$$

where, a = spin parameter

1.2.8 Existence of Magnetic Field

Since the motion of charges always produces a current, and hence the current links always with a field, called the magnetic field. It is represented by Maxwell-Ampere law(Fleisch 2008).

$$\oint \mathrm{B.dl} = \mu_0 \mathrm{i} + \mu_0 \epsilon_0 \frac{\mathrm{d}}{\mathrm{dt}} \int \mathrm{E.ds} \tag{1.6}$$

1.2.9 Accretion Disc

An accretion disk(Nowak and Wagoner 1991) is a nearly flat(means thickness is negligible compared to the radius) disc-like structure formed by the orbital motion of diffused material around a supermassive black hole. In this process, the falling material due to gravity inward to the central engine causes friction, making the disc hotter, which finally emits electromagnetic radiation over a certain frequency range. This is responsible for making the astrophysical jets around the supermassive black hole.

Chapter 2

Process of extraction of jet energy

AGN jets may be possibly powered by magnetic fields that extract either the energy of the accreting matter (Blandford- Payne(B-P) process)(Blandford and Payne 1982) or the rotational energy of the spinning black hole itself (Blandford–Znajek (B-Z) process)(Blandford and Znajek 1977). There is still a need to observe the launching process of the relativistic jets in AGN due to a lack of observational signature.

2.1 Extraction of rotational energy through the Penrose process

According to this process(Penrose and Floyd 1971), a falling particle towards the ergosphere region which is not crossed the event horizon gets split into two parts in such a way that one of them has positive energy and the other has negative energy that falls into a black hole, in this process the particle of positive energy escape out with higher energy than its initial.

Suppose particle A enters into the ergosphere region of a Kerr black Hole. It splits into particles B and C. Consequently (given the assumptions that energy conservation still holds for which one of the particles "c" is allowed to have negative energy), particle 'B' can exit the ergosphere with more energy than particle 'A'. In contrast, particle 'C' goes into the black hole, i.e., $E_A = E_B + E_C$ and say

$E_C < 0$, then...$E_B > E_A$.
Although in the magnetic Penrose process, it has been supported that the emerging particles also carry charges that provide the electromagnetic radiation(Poynting vector) for making this process more efficient.

2.2 Blendford-Znajek Process

Roger Blandford proposed this model, and Roman Znajek, in 1977, described an efficient process of astrophysical jet launched by a supermassive rotating black hole. This model(Blandford and Znajek 1977) explains the extraction of rotational energy through electromagnetic interaction. The process is performed by twisting of Poynting energy flux of magnetic fields arising from the accretion disc to the pole by frame-dragging effect, created by spin (which have the main role of angular momentum) of SMBH. This gives rise to a huge potential difference from the equator to the pole. Hence, for Blandford -Znajek model to be operative, there should exist a force-free magnetosphere.
Hence, on the dependence of certain parameters to launch a jet, the expression should be (Dadhich et al. 2018):

$$P_{BZ} = \frac{1}{32\Omega_H^2}\left[\omega(\Omega_H - \omega)\right] B_H^2 R_H^2 a^2 c \tag{2.1}$$

The maximum power from the black hole may be extracted when $\Omega_H = 2\omega$, for a rotating black hole. So the maximum B-Z power can be expressed in the from of $P_{BZ} = \frac{1}{128} B_H^2 R_H^2 a^2 c$ erg/sec. Putting the value of $R_H = m\left(1 + (1 - a^2)^{1/2}\right)$ Where, $m = GM/c^2$.
Therefore, the maximum Blandford-Znajek power can be expressed in terms of the dependence of Magnetic fields, Spin parameter and Mass of SMBHs.

$$P_{BZ} \sim 5 \times 10^{43} a^2 \left[1 + (1 - a^2)^{1/2}\right]^2 \left(\frac{M}{10^8 M_\odot}\right)^2 \left(\frac{B}{10^4 G}\right)^2 \text{ergs/sec.} \tag{2.2}$$

A mathematical variation can be plotted between spin parameter(on the x-axis) and Luminosity(on the Y-axis) from this equation. And Here, it found that Luminosity is the maximum for the spin parameter value of about 0.9.

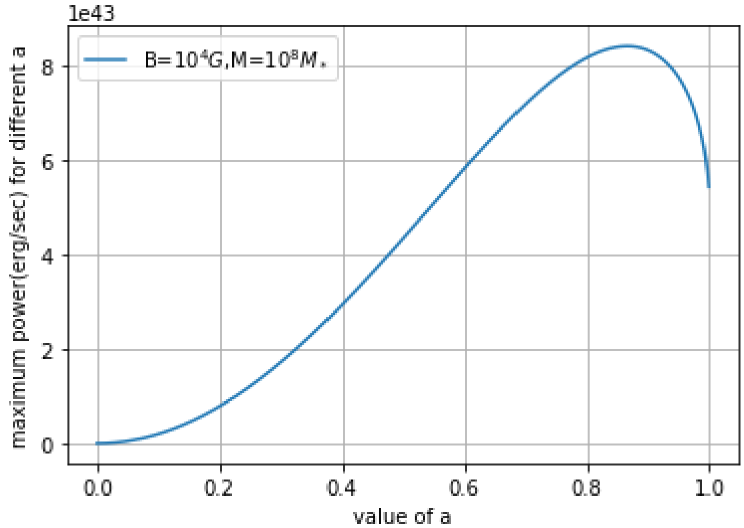

Figure 2.1: The spin parameter ranges from 0 to 1, and it is evident from the eq.(2.2) that the maximum power is extracted at $a \sim 0.9$.

Now, we can predict the magnetic field at max spin for the black hole surroundings (ergosphere), considering that the B-Z process supports the brightest flares from Blazars.

Hence the max power is finally be

$$\mathrm{P_{BZ}} = 8.35 \times 10^{43} \left(\frac{\mathrm{M}}{10^8 \mathrm{M}_\odot}\right)^2 \left(\frac{\mathrm{B}}{10^4 \mathrm{G}}\right)^2 \tag{2.3}$$

2.3 Magnetic field strengths

2.3.1 Eddington magnetic strength

In the case of standard disk, the maximum local equipartition condition can characterize the magnetic strength near gravitational radius(r_g). i.e., It's a balance of magnetic stress energy with the radiation (mathematically, given by $B^2/8\pi = T^4\mathrm{eff}/c$).

Now, accretion flow is the process that is governed by the balance between gravitational heating and cooling. Therefore its structure entirely depends on what kind of heating and cooling process have been followed that are dominated. In classical model (King 2012), this is generally referred to as a standard accretion disc model, where it is assumed geometrically flat (H << r) as compared to their thickness.

The temperature appeared in the above equation can be solved for the different case of the accretion process, for a viscous(frictional)stress that is the result of the conversion of gravitational potential energy into heat, locally in the form of thermal black body spectrum(here, advection process is not considered). The energy flux per unit surface area for this process can be expressed as

$$F(r) = \pi \int B_\nu T_{\text{eff}} d\nu = \sigma T_{\text{eff}}^4(r)$$

Here,final characteristic effective temperature can be expressed as

$$T_{\text{eff}} = 6.3 \times 10^5 \left(\frac{\dot{M}}{\dot{M}_{\text{Edd}}}\right)^{1/4} \left(\frac{10^8 M_\odot}{M}\right)^{1/4} \left(\frac{r_{\text{s}}}{r}\right)^{3/4} \left(1 - \sqrt{\frac{r_{\text{in}}}{r}}\right)^{1/4} \tag{2.4}$$

where, r_{s} = Schwarzschild radius

r_{in} = radius of inner edge

For the accretion rate is equal to Eddington mass accretion, it will correspond to Eddington magnetic strength and can be expressed as

$$B_{\text{Edd}} = 4.4 \times 10^4 \left(\frac{10^8 M_\odot}{M}\right)^{1/2} G \tag{2.5}$$

2.3.2 Critical magnetic strength

Since Ampere's and Faraday's laws are basic rules of physics, that shows how the magnetic fields are associated with moving charges. Hence, to follow the Blandford-Znajek mechanism the must exist a force-free(means gravitational and inertial forces are neglected, also called the massless limit of MHD) magnetosphere around the rotating black hole dominated by a magnetic and electric stress.

For a Kerr black hole immersed in asymptotically uniform magnetic fields B_0, the flux generated in the upper half of part of the magnetosphere is given by $\Phi = 4\pi B_0 M(r_H - m)$. This suggests a huge voltage difference between the horizon and pole.
Mathematically,

$$\Delta V \approx 10^{12} a \left(\frac{M}{10M_\odot}\right)\left(\frac{B_0}{10^4 G}\right) \text{Volts} \tag{2.6}$$

The equation describes massive black holes, having masses range 10^8 to 10^9 times solar masses, which can accelerate the stray electrons to a large value of the Lorentz factor, and the collision of these electrons with photons or charges of opposite sign create the cascade of electron-positron pair. Hence, to follow that process, there must exist a magnetic field to provide the direction for the motion of these charged particles during the collision, which needs the existence of a least critical strength of magnetic fields; otherwise, charges can leave the magnetosphere during motion at such a huge acceleration. That is mathematically(Blandford and Znajek 1977) given by

$$B_c \approx 6.2 \times 10^4 . a^{-3/4} \left(\frac{10M_\odot}{M}\right)^{1/2} \tag{2.7}$$

Chapter 3

Estimation of various parameters of black hole

3.1 List of sources of Blazars

Sources are taken from the SDSS DR7 Quasar list that is in the first Fermi sample.
The columns of the table containing
(1) Name,
(2) Logarithm of Black hole mass(in the form of the solar mass), and
(3) Luminosity observed over the first 11 months by Fermi-LAT operation.

table 1		
Source Name	$\log(M/M_{\odot})$	$L_{\gamma} \times 10^{45}$ erg/s
CGRaBS J0011+0057	8.95	217.51
B3 0307+380	8.23	54.97
B2 0743+25	9.59	3849.95
OJ 535	9.42	643.44
B2 0827+24	9.01	227.73
PKS 0906+01	9.32	462.35
0917+444	9.25	8261.87
0917+62	9.37	349.93
B2 0920+28	8.80	52.06
CGRaBS J0937+5008	8.29	4.59
CGRaBS J0941+2728	8.68	119.81
CRATES J0946+1017	8.52	639.52
CGRaBS J0948+0022	7.77	101.32
B2 0954+25A	9.34	32.10
4C +55.17	8.96	453.58
CRATES J1016+0513	9.11	2002.10
B3 1030+415	8.65	145.07
CRATES J1112+3446	9.04	583.93
CRATES J1117+2014	8.62	1.14
B2 1144+40	8.98	124.91
4C +29.45	9.18	196.10
CRATES J1208+5441	8.67	333.08
CRATES J1209+1810	8.94	40.69
4C +04.42	8.24	169.22
4C +21.35	8.87	29.89
CRATES J1228+4858	9.22	468.20
CRATES J1239+0443	8.67	1418.40

Source Name	$\log(M/M_{\odot})$	$L_{\gamma} \times 10^{45}$ erg/s
B2 1255+32	8.74	27.59
B2 1308+32	8.80	497.26
B2 1315+34A	9.29	55.36
CGRaBS J1321+2216	8.42	58.82
B2 1324+22	9.24	519.85
B3 1330+476	8.56	18.89
B2 1348+30B	8.69	22.73
PKS 1434+235	8.44	110.86
PKS 1502+106	9.64	22563.8
PKS 1509+022	8.84	3.98
PKS 1546+027	8.61	22.16
4C +05.64	9.38	209.33
PKS 1551+130	9.10	1003.15
4C +10.45	8.64	361.88
B2 1611+34	9.12	95.51
CRATES J1616+4632	8.44	93.91
4C +38.41	9.53	3420.04
CRATES J2118+0013	7.93	6.23
PKS 222708	8.95	2464.28

These datas are collected from https://academic.oup.com/view-large/20320708

3.2 Estimation of Luminosity for these sources

3.2.1 Doppler boosting problem

Doppler boosting (also known as Relativistic beaming, or the headlight effect) is the process by which relativistic effects modify the apparent luminosity of emitting matter that is moving nearly speed the speed of light.(Pei et al. 2020) which gives a way to choose the Doppler values for various γ ray sources of AGN and hence for Blazar.

For the average value of the lower limit of Doppler factor on γ-ray for which γ-ray emissions are strongly beamed, FRSQs and BL-Lacs have $<\delta_{\gamma}|\mathrm{FSRQ}> = 6.87\pm4.07$ and $<\delta\gamma|\mathrm{BL\ Lac}> = 4.31\pm2.97$ respectively.

Here, the average value of the Doppler factor can be chosen based on sources luminosity. Accordingly, for greater the order of 10^{47}erg/s. Its minimum value can be chosen as 6.87±4.07

and for lower the order of 10^{47}erg/s, its minimum value 4.31±2.97.

3.2.2 Photon index problem

In astronomy, photon index is defined as degree of dependence of frequency with the radiative flux of the sources. For a given frequency ν and radiative flux density S_{ν}, photon index α_p is correlated by

$$\mathrm{S}_{\nu} \propto \nu^{\alpha_{\mathrm{p}}-1} \tag{3.1}$$

Generally, α represent spectral index and α_p represent photon index and these are correlated as $\alpha = \alpha_p - 1$.

The variation of photon index and luminosity can be approximated to the paper (Ajello et al. 2020).

and hence from the graphical estimation(fig:3.1), the best possible value of photon index can be chosen to to resolve the observed luminosity.

3.2.3 Relation between observed and theoretical(B-Z) luminosity

Since the observed Luminosity is generally Doppler boosted, and hence it becomes modified from the true Luminosity, it can be resolved by the mathematical relation,

$$\mathrm{L}_{\mathrm{obs}} = \epsilon\delta^{(3+\alpha_{\mathrm{p}})}\mathrm{L}_{\mathrm{BZ}} \tag{3.2}$$

Where ϵ is an observation factor. Since flux would be drop with jet distance, it is assumed that observed flux is 10% of real jet power.

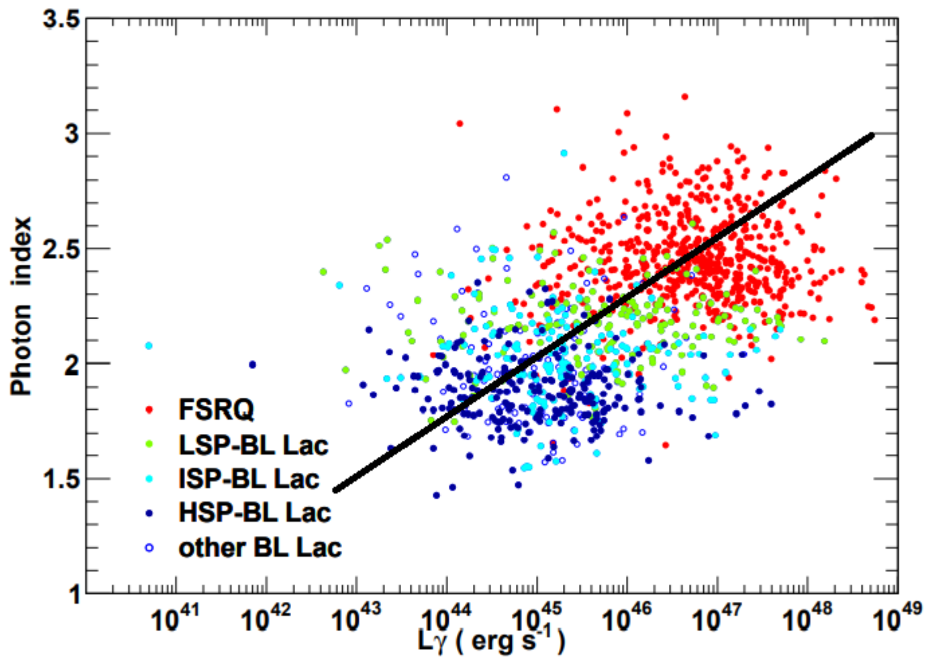

this shows Photon index vs. gamma-ray luminosity for the different blazar classes and subclasses. Error bars have been omitted for clarity. The mean photon-index uncertainties are 0.08 and 0.10 for FSRQs and BL Lacs respectively.

Figure 3.1: The result is taken from arXiv:1905.10771(Ajello et al. 2020), through the fermi lat collaboration.

3.3 Estimation of Magnetic field strength

Blendford-Znajek model describes through the equation(2.2), and it can be rearranged as,

$$\sqrt{\frac{\mathrm{P_{BZ}}}{5\times10^{43}\mathrm{erg/s}}}\left(\frac{10^8\mathrm{M_\odot}}{\mathrm{M}}\right)=\mathrm{a}(1+\sqrt{1-\mathrm{a}^2})\left(\frac{\mathrm{B_P}}{10^4\mathrm{G}}\right) \tag{3.3}$$

Hence for a source, R.H.S of the equation describes the two terms. Where first is for spin parameter and second is for the magnetic field, although maximizing the spin terms would minimize the magnetic fields, thus on analysing for a source like 3C454.3(Bonnoli et al. 2010)
where, $L_{obs} = 5.01\times10^{48}$ erg/s and $\log(M/M_\odot) = 8.7$
Their photon index α_p= 2.5 can be used by graph in fig(3.1) also by using eq(3.3).
Also the maximum value of spin would be nearly at a = 0.9, and hence the minimum value of magnetic fields strength for the force-free magnetosphere can be calculated by the observed data.
i.e.,$B = 0.76\times10^4$Gauss.
A similar process can be followed for all sources listed in the table above, and an empirical equation can be estimated for a general mass dependence of a SMBH.

And hence on the logarithm scale, the empirical equation can be best estimated as,

$$\log\mathrm{B} = 13.58 - 2.35\log\left(\frac{\mathrm{M}}{\mathrm{M_\odot}}\right)^{0.68} \tag{3.4}$$

The graph shows a blue straight line that is the boundary of Eddington Magnetic field strength, therefore we can estimate a mass limit of SMBH that exists in blazar. Hence minimum mass limit can be traced by extra plotting in this graph. The lower limit of mass of an SMBH for a Blasar is found close to $10^6M_\odot$ that mentioned value(in section 2.) (RIEGER 2011), which agrees with the graphical value.

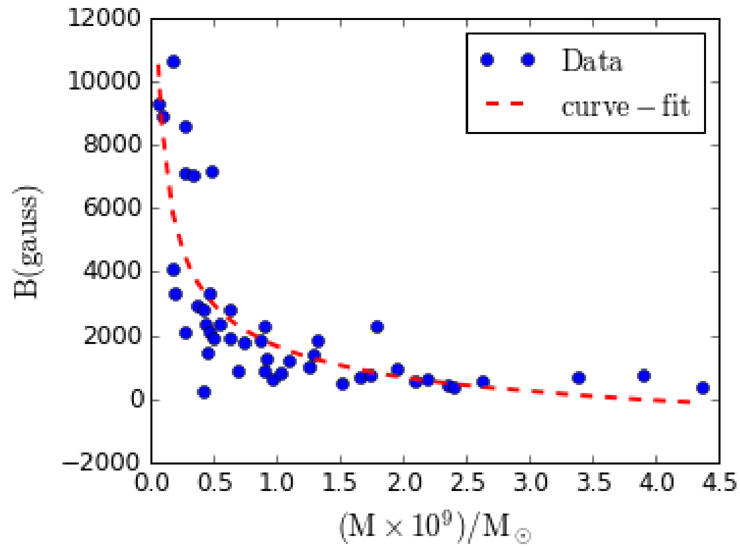

Figure 3.2: The graph represents the variation of magnetic field of lower strength as spin is taken maximum for all the sources listed in table 1.

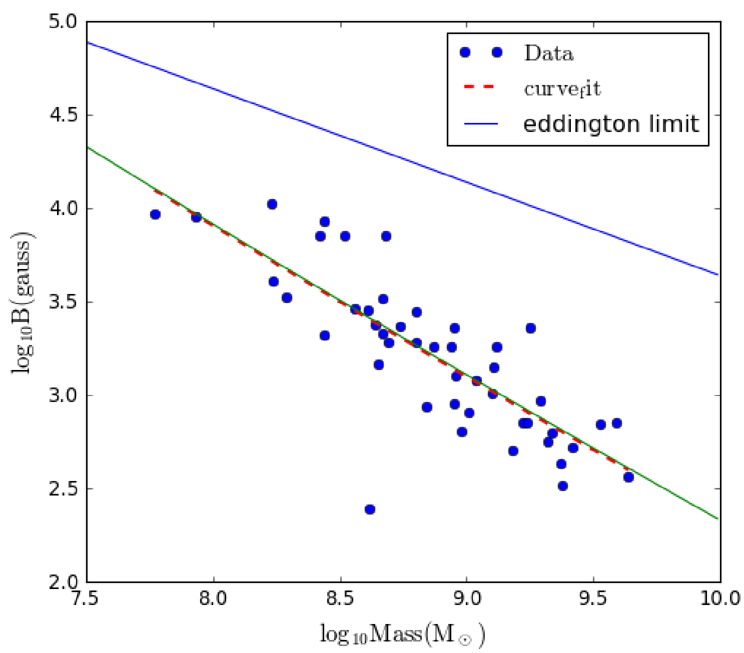

Figure 3.3: Graph is showing the variation of magnetic field with masses of SMBH on the logarithm scale

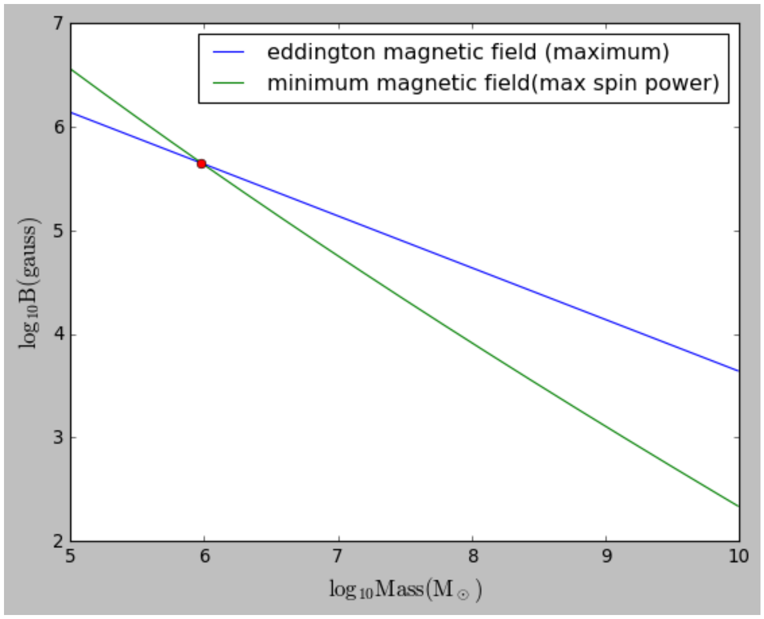

Figure 3.4: Figure shows the Eddington(max) and lower magnetic field, and behind the cross point. It can't exist.

3.4 Estimation of minimum spin parameter

Most of the Blazars are hosted by elliptical galaxies(Urry et al. 2000), and the number of stars in the galaxies and their arrangement are nearly the same; hence the action of spin on the central SMBH should be followed by the gravity of these stars. There should be a mass dependence parameter relation with the minimum spin(unperturbed). Here, in table: 2 only radio-loud sources(Urry and Padovani 1995) are chosen to distinguish the radio-loud and radio-quiet AGN. However, the minimum spin parameter can be calculated by the equation(2.2) where the magnetic field should follow by Eddington(maximum) case to estimate the minimum spin. The list of radio-loud AGNs is distinguished from table 1.

table 2		
Source Name	$\log(M/M_{\odot})$	$L_{\gamma} \times 10^{45}$ erg/s
B3 0307+380	8.23	54.97
B2 0743+25	9.59	3849.95
OJ 535	9.42	643.44
PKS 0906+01	9.32	462.35
B2 0920+28	8.80	52.06
CRATES J0946+1017	8.52	639.52
B2 0954+25A	9.34	32.10
4C +55.17	8.96	453.58
CRATES J1016+0513	9.11	2002.10
CRATES J1112+3446	9.04	583.93
CRATES J1209+1810	8.94	40.69
4C +21.35	8.87	29.89
CRATES J1228+4858	9.22	468.20
CRATES J1239+0443	8.67	1418.40
B2 1255+32	8.74	27.59
B2 1308+32	8.80	497.26
B2 1315+34A	9.29	55.36
CGRaBS J1321+2216	8.42	58.82
B2 1324+22	9.24	519.85
PKS 1502+106	9.64	22563.8
PKS 1546+027	8.61	22.16
PKS 1551+130	9.10	1003.15
B2 1611+34	9.12	95.51
CRATES J1616+4632	8.44	93.91
4C +38.41	9.53	3420.04
PKS 222708	8.95	2464.28

Solving for minimum spin value for these sources by using equation(2.2),

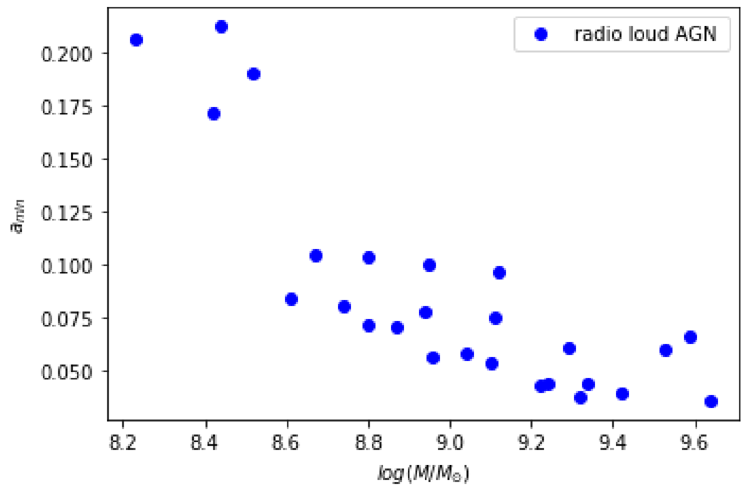

Figure 3.5: Graph is shown for radio loud AGNs as min spin on Y-axis and mass on X-axis.

the variation of min spin with mass is traced in the fig(3.6).

This variation can be mathematically represented as,

$$\mathrm{a_{min}} = \frac{5.55 \times 10^{10}}{\left[\log\left(\frac{\mathrm{M}}{\mathrm{M}_{\odot}}\right)\right]^{12.45}} \tag{3.5}$$

Now, for a mass range 10^8 to $10^{10} M_{\odot}$ min spin can be estimated if a source has known these two values and if the observed spin value will be lower than that of estimated through mass, then they must be the radio-quiet source.

3.5 Estimation of Mass and Luminosity phase diagram

The phase diagram for Mass and Luminosity of listed sources (in table 1) can be estimated with the help of Eddington luminosity(for maximum boundary) and the possible power of jet by Blendford-Znajek equation that is conditioned by minimum

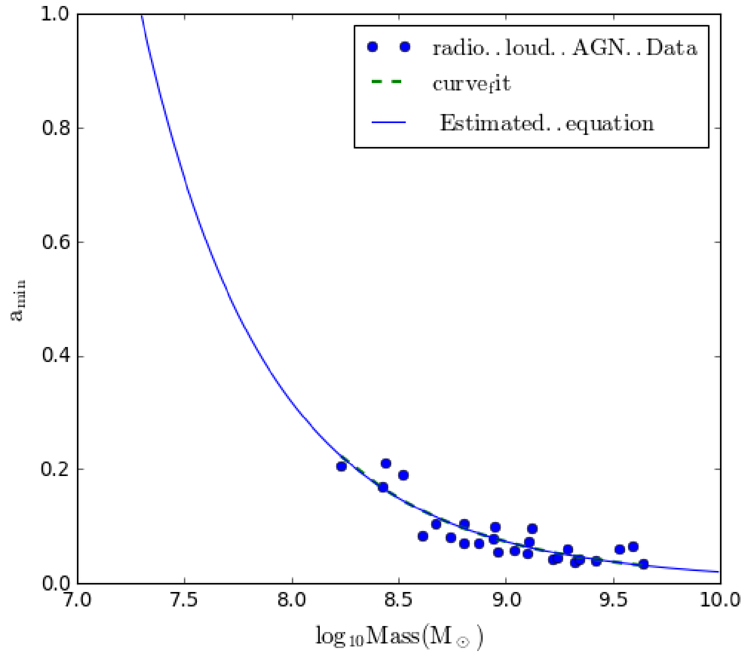

Figure 3.6: An estimated line is fitted to trace an equation for these variation.

spin and minimum magnetic field obtained by fitting equation through observation (for minimum boundary).
By using equation(3.3) and putting the fitted equation of min spin(3.5) and min magnetic strength(3.4), the variation pattern is shown here.

Now, On clubbing both conditions and observation recorded in the table: 1, the phase-space for mass and luminosity can be traced.

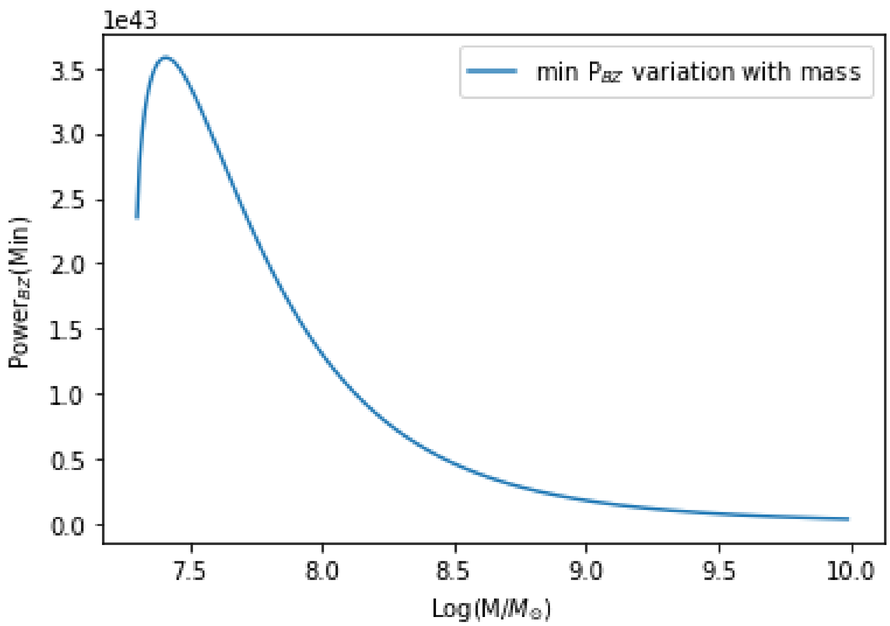

Figure 3.7: Variation of minimum power with mass by the Blendford-Znajek and Eddington equation.

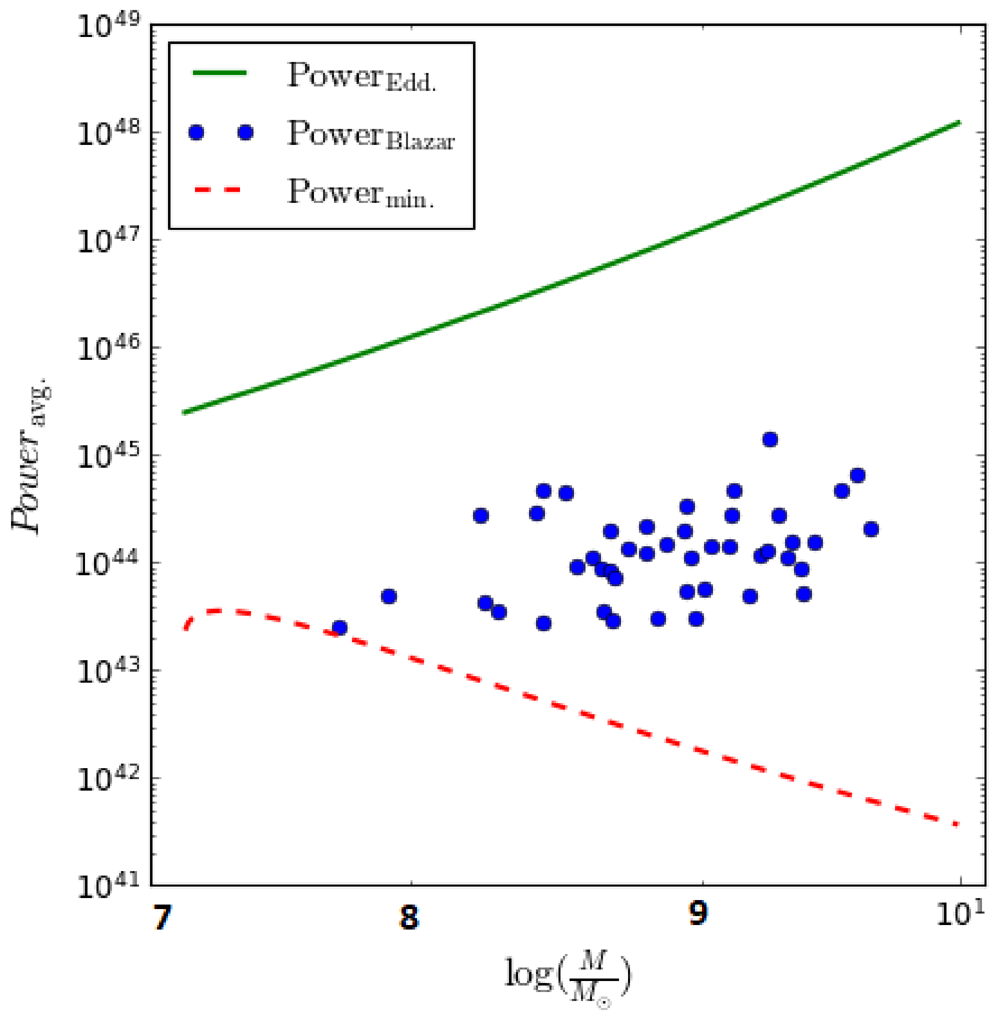

Figure 3.8: The graph showing the phase-space of Blazars, where all lies in the region bounded by upper(Eddington) and lower(Blendford-Znajek at min power case) according to this representation all Blasars would belong in between this two region in their life span.

Chapter 4

Results and Conclusions

4.1 Results:

- Minimum possible magnetic strength for magnetosphere that pointing towards launched jet from accretion disc at max spin parameter ~ 0.9 is related with SMBH mass as

$$\log \mathrm{B} = 13.58 - 2.35 \log \left(\frac{\mathrm{M}}{\mathrm{M}_{\odot}} \right)^{0.68} \tag{4.1}$$

- Minimum spin parameter at maximum possible magnetic field(Eddington case) of SMBH is related with their mass as

$$\mathrm{a}_{\mathrm{min}} = \frac{5.55 \times 10^{10}}{\left[\log \left(\frac{\mathrm{M}}{\mathrm{M}_{\odot}} \right) \right]^{12.45}} \tag{4.2}$$

- Combining these above two equation for the Blendford-Znajek power jet equation, that gives minimum power of the jet, that is shown in graphs(fig:3.7)

- The phase-space(traced in fig: 3.8) is represented for mass Vs luminosity, contains 46 sources of blazars, which is bounded by min and max luminosity lines.

4.2 Conclusions:

According to the above results, we can conclude that;

- Heavier the mass of SMBHs result in lower spin parameters and hence, magnetic strength gets also lower with it.
- Heavier SMBHs have wider luminosity range variation(shown in phase-space), although the spin parameter range is the same.
- all results are based only on the Blandford-Znajek model and the sources taken from Fermi-LAT data.

Bibliography

[1] M. Ajello et al. In: *The Astrophysical Journal* 892.2 (2020), p. 105. ISSN: 1538-4357. DOI: 10.3847/1538-4357/ab791e. URL: http://dx.doi.org/10.3847/1538-4357/ab791e.

[2] M. Baldwin. In: *Physics Today* 74.5 (2021), pp. 26–33. DOI: 10.1063/PT.3.4747. eprint: https://doi.org/10.1063/PT.3.4747. URL: https://doi.org/10.1063/PT.3.4747.

[3] V. Beckmann and C. SHRADER. In: July 2013, p. 069. DOI: 10.22323/1.176.0069.

[4] R. D. Blandford and D. G. Payne. In: 199 (June 1982), pp. 883–903. DOI: 10.1093/mnras/199.4.883.

[5] R. D. Blandford and R. L. Znajek. In: 179 (May 1977), pp. 433–456. DOI: 10.1093/mnras/179.3.433.

[6] R. D. Blandford and R. L. Znajek. In: *Monthly Notices of the Royal Astronomical Society* 179.3 (July 1977), pp. 433–456. ISSN: 0035-8711. DOI: 10.1093/mnras/179.3.433. eprint: https://academic.oup.com/mnras/article-pdf/179/3/433/9333653/mnras179-0433.pdf. URL: https://doi.org/10.1093/mnras/179.3.433.

[7] G. Bonnoli et al. In: (May 2010).

[8] S. Chandrasekhar. *The Mathematical Theory of Black Holes*. New York: Oxford University Press, 1992.

[9] N. Dadhich et al. In: *Monthly Notices of the Royal Astronomical Society: Letters* 478.1 (Apr. 2018), pp. L89–L94. ISSN: 1745-3925. DOI: 10.1093/mnrasl/sly073. eprint: https://academic.oup.com/mnrasl/article-pdf/478/1/L89/25051074/sly073.pdf. URL: https://doi.org/10.1093/mnrasl/sly073.

[10] S. Deser and J. Franklin. In: *American Journal of Physics* 73.3 (2005), 261–264. ISSN: 1943-2909. DOI: 10.1119/1.1830505. URL: http://dx.doi.org/10.1119/1.1830505.

[11] D. Fleisch. Student's Guides. Cambridge University Press, 2008. ISBN: 9781139468473. URL: https://books.google.co.in/books?id=I-x1MLny6y8C.

[12] R. P. Kerr. In: *Phys. Rev. Lett.* 11 (5 1963), pp. 237–238. DOI: 10.1103/PhysRevLett.11.237. URL: https://link.aps.org/doi/10.1103/PhysRevLett.11.237.

[13] A. King. 2012. arXiv: 1201.2060 [astro-ph.HE].

[14] A. J. van Marle, S. P. Owocki, and N. J. Shaviv. In: (2008). DOI: 10.1063/1.2905555. URL: http://dx.doi.org/10.1063/1.2905555.

[15] I. Morison. Wiley, 2013. ISBN: 9781118681527. URL: https://books.google.co.in/books?id=Fh_yo8Jv7t8C.

[16] M. A. Nowak and R. V. Wagoner. In: 378 (Sept. 1991), p. 656. DOI: 10.1086/170465.

[17] J. R. Oppenheimer and H. Snyder. In: *Phys. Rev.* 56 (5 1939), pp. 455–459. DOI: 10.1103/PhysRev.56.455. URL: https://link.aps.org/doi/10.1103/PhysRev.56.455.

[18] Z. Pei et al. In: *Publications of the Astronomical Society of Australia* 37 (2020). ISSN: 1448-6083. DOI: 10.1017/pasa.2020.30. URL: http://dx.doi.org/10.1017/pasa.2020.30.

[19] R. Penrose and R. M. Floyd. In: *Nature Physical Science* 229.6 (Feb. 1971), pp. 177–179. DOI: 10.1038/physci229177a0.

[20] F. M. RIEGER. In: *International Journal of Modern Physics D* 20.09 (2011), 1547–1596. ISSN: 1793-6594. DOI: 10.1142/s0218271811019712. URL: http://dx.doi.org/10.1142/S0218271811019712.

[21] T. Sauer. 2014. arXiv: 1312.4068 [physics.hist-ph].

[22] A. M. M. Scaife and F. Porter. In: *Monthly Notices of the Royal Astronomical Society* 503.2 (2021), 2369–2379. ISSN: 1365-2966. DOI: 10.1093/mnras/stab530. URL: http://dx.doi.org/10.1093/mnras/stab530.

[23] G. A. Shields. In: *Publications of the Astronomical Society of the Pacific* 111.760 (1999), 661–678. ISSN: 1538-3873. DOI: 10.1086/316378. URL: http://dx.doi.org/10.1086/316378.

[24] C. M. Urry and P. Padovani. In: *Publications of the Astronomical Society of the Pacific* 107 (1995), p. 803. ISSN: 1538-3873. DOI: 10.1086/133630. URL: http://dx.doi.org/10.1086/133630.

[25] C. M. Urry et al. In: *The Astrophysical Journal* 532.2 (2000), 816–829. ISSN: 1538-4357. DOI: 10.1086/308616. URL: http://dx.doi.org/10.1086/308616.

[26] R. Wald. University of Chicago Press, 2010. ISBN: 9780226870373. URL: https://books.google.co.in/books?id=9S-hzg6-moYC.